JACS ARTICLES

Published on Web 03/19/2010

Oxygen-Isotope Exchange Rates for Three Isostructural Polyoxometalate Ions

Eric M. Villa, C. André Ohlin, and William H. Casey*

Departments of Chemistry and Geology, University of California, Davis, California 95616

Received January 19, 2010; E-mail: whcasey@ucdavis.edu

Abstract: We compare oxygen-isotope exchange rates for all structural oxygens in three polyoxoniobate ions that differ by systematic metal substitutions of Ti(IV) → Nb(V). The $[H_xNb_{10}O_{28}]^{(6-x)-}$, $[H_xTiNb_9O_{28}]^{(7-x)-}$, and $[H_xTi_2Nb_8O_{28}]^{(8-x)-}$ ions are all isostructural yet have different Brønsted properties. Rates for sites within a particular molecule in the series differ by at least $\sim 10^4$, but the relative reactivities of the oxygen sites rank in nearly the same relative order for all ions in the series. Within a single ion, most structural oxygens exhibit rates of isotopic exchange that vary similarly with pH, indicating that each structure responds as a whole to changes in pH. Across the series of molecules, however, the pH dependencies for isotope exchanges and dissociation are distinctly different, reflecting different contributions from proton- or base-enhanced pathways. The proton-enhanced pathway for isotope exchange dominates at most pH conditions for the $[H_xTi_2Nb_8O_{28}]^{(8-x)-}$ ion, but the base-enhanced pathways are increasingly important for the $[H_xTiNb_9O_{28}]^{(7-x)-}$ and $[H_xNb_{10}O_{28}]^{(6-x)-}$ structures at higher pH. The local effect of Ti(IV) substitution could be assessed by comparing rates for structurally similar oxygens on each side of the $[H_xTiNb_9O_{28}]^{(7-x)-}$ ion and is surprisingly small. Interestingly, these nanometer-size structures seem to manifest the same general averaged amphoteric chemistry that is familiar for other reactions affecting oxides in water, including interface dissolution by proton- and hydroxyl-enhanced pathways.

Introduction

Many questions about molecular-scale reactions that occur at the mineral−water interface cannot yet be confidently answered. These include the following: (1) Which oxygen(s) in a given structure will exchange most rapidly with water and how fast? (2) To what extent do these reactions proceed via concerted motions of many atoms? (3) How broadly does protonation affect the reactivity of an oxide structure? (4) To what extent can one use a truncated structure of an extended solid in ab initio simulation and capture the essential chemistry?

In spite of advances, it is yet unclear what functional groups are present at an interface, how they arrange, how they interact with each other and with solutes, and how rapidly they undergo ligand exchanges in this reaction.[1] Research from the polyoxometalate (POM) community could help. POMs make up a broad class of compounds with a wide range of applications.[2−5] However, unlike the oxide interfaces, the structures of many POMs in solution are relatively well-known and spectroscopic tools exist to detail reactions in solution that are impossible for extended structures.[6−15] For some classes of POMs, isomerization and dissociation of the molecule has been followed in situ.[16] One can also make targeted substitutions that modify bonding in the structure and follow the effect on reactivity.[17,18] Thus, POMs have long been used to complement direct study of oxide interfaces.[19−22]

Here we directly address questions 1−4 above. We compare oxygen-isotope exchange rates a series of molecules, the $[H_xNb_{10}O_{28}]^{(6-x)-}$, $[H_xTiNb_9O_{28}]^{(7-x)-}$, and $[H_xTi_2Nb_8O_{28}]^{(8-x)-}$ ions, that differ only by targeted Ti(IV) → Nb(V) substitutions (for clarity, these ions will be identified as Nb_{10}, $TiNb_9$, and Ti_2Nb_8, respectively, throughout the paper). Isotope exchange rate data were previously reported for the decaniobate ion Nb_{10}

(1) Catalano, J. G.; Fenter, P.; Park, C. *Geochim. Cosmochim. Acta* **2009**, *73*, 2242.
(2) Pope, M. T.; Müller, A. *Polyoxometalate Chemistry From Topology via Self Assembly to Applications*; Springer: New York, 2001; 427 pp.
(3) Pope, M. T.; Müller, A. *Angew. Chem., Int. Ed. Engl.* **1991**, *30*, 34.
(4) Rhule, J. T.; Hill, C. L.; Judd, D. A. *Chem. Rev.* **1998**, *98*, 327.
(5) Long, D. L.; Burkholder, E.; Cronin, L. *Chem. Soc. Rev.* **2007**, *36*, 105.
(6) Filowitz, M.; Klemperer, W. G.; Messerle, L.; Shum, W. *J. Am. Chem. Soc.* **1976**, *98*, 2345.
(7) Klemperer, W. G. *Angew. Chem., Int. Ed. Engl.* **1978**, *17*, 246.
(8) Filowitz, M.; Ho, R. K. C.; Klemperer, W. G.; Shum, W. *Inorg. Chem.* **1979**, *18*, 93.
(9) Fedotov, M. A.; Maksimovskaya, R. I.; Kazanskii, L. P. *React. Kinet. Catal. Lett.* **1981**, *16*, 185.
(10) Besecker, C. J.; Klemperer, W. G.; Maltbie, D. J.; Wright, D. A. *Inorg. Chem.* **1985**, *24*, 1027.
(11) Howarth, O. W.; Kelly, P. *Dalton Trans.* **1990**, 81.
(12) Murmann, R. K.; Giese, K. C. *Inorg. Chem.* **1978**, *17*, 1160.
(13) Comba, P.; Helm, L. *Helv. Chim. Acta* **1988**, *71*, 1406.
(14) Day, V. W.; Klemperer, W. G.; Maltbie, D. J. *J. Am. Chem. Soc.* **1987**, *109*, 2991.
(15) Howarth, O. W.; Jarrold, M. *Dalton Trans.* **1978**, *5*, 503.
(16) Cowan, J. J.; Bailey, A. J.; Heintz, R. A.; Do, B. Ti.; Hardeastle, K. I.; Hill, C. L.; Weinstock, I. A. *Inorg. Chem.* **2001**, *40*, 6666.
(17) Klemperer, W. G.; Shum, W. *J. Am. Chem. Soc.* **1976**, *98*, 8291.
(18) Casey, W. H. *Chem. Rev.* **2006**, *106*, 1.
(19) Alam, T. M.; Nyman, M.; Cherry, B. R.; Segall, J. M.; Lybarger, L. E. *J. Am. Chem. Soc.* **2004**, *126*, 5610.
(20) Black, J. R.; Nyman, M.; Casey, W. H. *J. Am. Chem. Soc.* **2006**, *128*, 14712.
(21) Anderson, T. M.; Rodriguez, M. A.; Bonhomme, F.; Bixler, J. N.; Alam, T. M.; Nyman, M. *Dalton Trans.* **2007**, *40*, 4517.
(22) Day, V. W.; Klemperer, W. G. *Science* **1985**, *228*, 533.

10.1021/ja100490n

and showed that the locus of base-enhanced dissociation was a μ_3-oxo near the central Nb(V).[23] This observation led to a hypothesis that dissociation could be suppressed by Ti(IV) for Nb(V) substitution near the μ_3-oxo. The ionic radii of the two metals are similar (60.5 versus 64.0 pm, respectively), but overbonding at the μ_3-oxo could be reduced by bonding to a metal with lower charge than Nb(V).[24,25] Accordingly, the dititanoniobate ion Ti_2Nb_8 was found to be much more stable to base-enhanced dissociation than Nb_{10}, but most interestingly, the pH dependencies for oxygen-isotope exchanges were inverted throughout the molecule at high pH.[23,24] Here we show why this substitution so profoundly affects rates of isotopic exchanges through a study of the monotitanoniobate ion $TiNb_9$ (Figure 1, top), with a single atom substitution.[26] The results confront directly the questions posed above about oxide mineral reactivities in general.

Experimental Section

Synthesis of ^{17}O-Enriched $[N(CH_3)_4]_7[TiNb_9O_{28}]$: The tetramethylammonium salt of monotitanoniobate ion, $[N(CH_3)_4]_7[TiNb_9O_{28}]$, was synthesized via a modification of the original method.[26] This modification allowed for ^{17}O enrichment of all structural oxygens in the $TiNb_9$ ion. A mixture of $N(CH_3)_4OH\cdot 5\ H_2O$ (305 mg), $Ti(OCH(CH_3)_2)_4$ (75 μL), and hydrous niobium oxide (500 mg) in $H_2{}^{17}O$ (40% ^{17}O from Isotec Laboratories, 4 mL) was reacted in a PTFE-lined autogenic pressure vessel at 200 °C in an oven for a minimum of 15 h. The resulting mixture was dried in vacuo to recover the $H_2{}^{17}O$, and the product was extracted from the solid residues with aliquots of ethanol, followed by extraction with aliquots of methanol. The ethanolic and methanolic fractions were dried separately in vacuo, yielding two batches of product in the form of a white powder. Characterization of the products by ESI-MS indicated that the batches were pure, save for the presence of some of the hexaniobate $[H_xNb_6O_{19}]^{(8-x)-}$ ion, which will be abbreviated to Nb_6. The discussion of bond lengths and bond angles for all three isostructural ions can be found in Ohlin et al.[26]

Synthesis of ^{17}O-Enriched $[N(CH_3)_4]_8[Ti_2Nb_8O_{28}]$: The previous study of the Ti_2Nb_8 ion employed the sodium salt, while studies involving the $TiNb_9$ or Nb_{10} ions employed the corresponding tetramethylammonium salts.[23,24] To investigate counterion effects, an ^{17}O-enriched mixture of $[N(CH_3)_4]_8[Ti_2Nb_8O_{28}]$ and $[N(CH_3)_4]_7[TiNb_9O_{28}]$ was also synthesized. To make the material, isotopically normal $[N(CH_3)_4]_8[Ti_2Nb_8O_{28}]$ was first prepared by reacting a mixture of hydrous niobium oxide (1.05 g), $Ti(OCH(CH_3)_2)_4$ (0.9 mL), and $N(CH_3)_4OH\cdot 5\ H_2O$ (1.5 g) at 150 °C in a PTFE-lined autogenic pressure vessel for 20 h. The resulting mixture of oil and solids was separated by centrifugation, and the solids were extracted with several aliquots of methanol while the oil was discarded. The combined methanolic extractions were placed in a beaker and allowed to evaporate over a period of a few days, yielding crystals of $[N(CH_3)_4]_8[Ti_2Nb_8O_{28}]$ (see Supporting Information for ESI-MS data). Four hundred milligrams of the $[N(CH_3)_4]_8[Ti_2Nb_8O_{28}]$ was dissolved in 2 mL of $H_2{}^{17}O$ (40% ^{17}O, from Isotec Laboratories), placed in a PTFE-lined autogenic pressure vessel, and heated at 150 °C for 6 days. The $H_2{}^{17}O$ was recovered by drying in vacuo, yielding a white powder of a mixture of ^{17}O-enriched $[N(CH_3)_4]_8[Ti_2Nb_8O_{28}]$ and $[N(CH_3)_4]_7[TiNb_9O_{28}]$ as determined by ESI-MS and ^{17}O NMR (see Supporting Information).

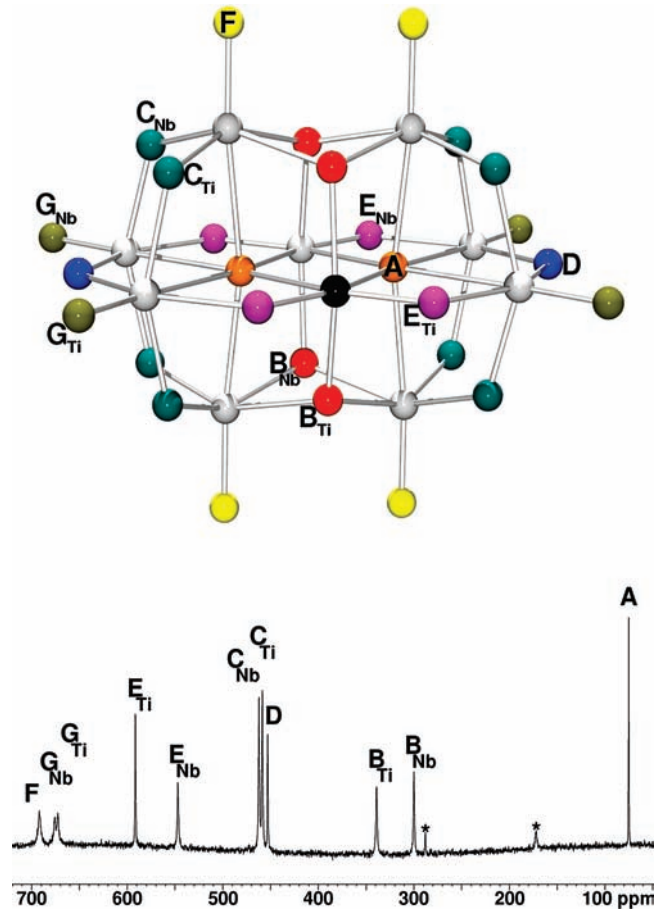

Figure 1. Top: Monotitanoniobate ion, $TiNb_9$, with color-coded oxygens (niobium is shown in gray, and titanium is shown in black). All oxygens labeled with a subscript "Ti" are on the titanium side of the molecule, whereas oxygens labeled with a subscript "Nb" are on the niobium side of the molecule. The labels are as follows: μ_6-oxo site A; μ_3-oxo sites B_{Nb} and B_{Ti}; μ_2-oxo sites D, C_{Ti}, C_{Nb}, E_{Nb}, and E_{Ti}; η-oxo sites G_{Ti}, G_{Nb}, and F. Bottom: ^{17}O NMR spectra of $TiNb_9$ ion at pH ~8.5, where the bulk water peak is set to zero. Two small impurity peaks, indicated with an asterisk, in the $TiNb_9$ spectrum are probably due to a small impurity of the $[Ti_{12}Nb_6O_{44}]^{10-}$ ion and carbonate ion, at ~288 and ~170 ppm, respectively. All four structural oxygens that are no longer symmetric in the $TiNb_9$ ion (site B μ_3-oxo, site C μ_2-oxo, site E μ_2-oxo, and site G η-oxo) are split into two separate signals.

^{17}O NMR: The solution-state ^{17}O NMR experiments were conducted with a 500 MHz Bruker Avance spectrometer located at the UCD NMR facility. This spectrometer is based on an 11.7 T magnet (ν_o = 67.8 MHz for ^{17}O) and is fitted with a 10 mm broadband probe. The ^{17}O NMR spectra were taken with single-pulse excitations using 20 μs pulses and recycle delays of 6 ms. The time-domain data were digitized at 8 kHz. A 0.3 M $TbCl_3$ solution was employed as an external intensity standard, which was included in the 10 mm NMR tube as a coaxial insert. Depending upon the sample concentration and rate of reaction, 5000−15 000 acquisitions were required to establish an adequate signal-to-noise ratio. The temperature was measured by replacing the sample with a copper-constantan thermocouple fitted into an NMR tube with an equal amount of water to that used in the experiments. The accuracy of the measured temperature was about ±0.1 °C. Peak positions are reported relative to the bulk water peak, which was assigned to 0 ppm.

Rate experiments were conducted by dissolving ~15 mg of the ^{17}O-enriched $[N(CH_3)_4]_7[TiNb_9O_{28}]$ into 2 mL of an isotopically normal solution containing a 50 mM pH buffer and 0.1 M $[N(CH_3)_4]Cl$. The ^{17}O NMR signal intensities for each structural oxygen decrease as the isotopically normal $H_2{}^{16}O$ exchanges with

(23) Villa, E. M.; Ohlin, C. A.; Balogh, E.; Anderson, T. M.; Nyman, M. D.; Casey, W. H. *Angew. Chem., Int. Ed.* **2008**, *47*, 4844.
(24) Villa, E. M.; Ohlin, C. A.; Rustad, J. R.; Casey, W. H. *J. Am. Chem. Soc.* **2009**, *131*, 16488.
(25) Nyman, M.; Criscenti, L. J.; Bonhomme, F.; Rodriguez, M. A.; Cygan, R. T. *J. Solid State Chem.* **2003**, *176*, 111.
(26) Ohlin, C. A.; Villa, E. M.; Fettinger, J. C.; Casey, W. H. *Dalton Trans.* **2009**, 2677.

the individual oxygen sites and were followed as a function of time to yield the rates of isotopic exchange.[20,23,24] Some small impurities are seen within the $TiNb_9$ ^{17}O NMR spectra: carbonate, the Nb_6 ion, and an unknown peak that could be from $[Ti_{12}Nb_6O_{44}]^{10-}$ ion.[20,27] Dissociation of the ion is easily detected as a decline in the signal intensity for the central μ_6-oxo site as it is exposed to the isotopically normal solution; it is otherwise constant in intensity. Other side reactions are also detected as a decline in the μ_6-oxo signal, which is sometimes simultaneous with growth of a new signal(s) in an adjacent region of the ^{17}O NMR spectrum. The μ_6-oxo signals for niobate ions are typically found in this region.

The protonation constants were measured in 0.1 M $[N(CH_3)_4]Cl$ that had been degassed with $N_{2(g)}$. The 5 mM $[N(CH_3)_4]_7[TiNb_9O_{28}]$ solution was initially titrated down to the lower limit in pH stability (pH ~6.5) with 0.01 M HCl in 0.1 M $[N(CH_3)_4]Cl$ and then titrated back with 0.01 M $[N(CH_3)_4]OH$ in 0.1 M $[N(CH_3)_4]Cl$. The pK_a values were identified from inflections and were assigned with assistance of the software CurTiPot, which is available from Prof. Gutz from the Instituto de Química Universidade de São Paulo.[28] Uncertainties were estimated from repeated measurements.

Results

In the $TiNb_9$ ion, a single Nb(V) is replaced by Ti(IV) at one of the central metal sites in the structure near the site B oxygen, which was found to be key in the base-enhanced dissociation of the Nb_{10} ion (Figure 1, top).[23,24] Correspondingly, the ^{17}O NMR spectrum (Figure 1, bottom) of the $TiNb_9$ ion generally resembles those of the Nb_{10} or Ti_2Nb_8 ions, but the reduced symmetry splits the signals from several of the structural oxygens into two separate signals (μ_3-oxo site B, μ_2-oxo site C, μ_2-oxo site E, and η-oxo site G); moreover, the magnitude of their separation correlates to their distance from the Ti(IV) substitution. The spectrum shows that there are two groups of oxygens split by this asymmetry: sites B and E have the largest separation and are directly bonded to the Ti(IV), whereas sites C and G are three bonds away from the Ti(IV) and have a much smaller separation (see Table S-2-2 in the Supporting Information for a comparison of chemical shifts for Nb_{10}, $TiNb_9$, and Ti_2Nb_8). The ^{17}O NMR spectrum indicates 11 structural oxygens in the $TiNb_9$ ion, rather than the seven structural oxygens in the Nb_{10} and Ti_2Nb_8 structures. To designate the oxygens, but maintain the same general labeling scheme used previously, a subscript is added to indicate whether the particular oxygen lies on the titanium (Ti) or niobium (Nb) side of the molecule (Figure 1).

The four μ_3-oxo (site B), eight μ_2-oxo (site C), four μ_2-oxo (site E), and four η-oxo (site G) signals are split into two groups according to whether they fall near or away from the site of substitution. The peak positions of the two μ_6-oxo (site A), two μ_2-oxo (site D), and four η-oxo (site F) are unaffected by the substitution as the oxygens within each of these classes remain symmetrically equivalent (Figure 1, bottom). The ^{17}O NMR peak positions for sites B_{Ti} and E_{Ti} are shifted downfield relative to sites B_{Nb} and E_{Nb}, but the opposite is observed for sites C and G. Sites C_{Nb} and G_{Nb} are shifted downfield relative to sites C_{Ti} and G_{Ti}. The separation of site G allows unequivocal assignment of this ^{17}O NMR peak. Previously, the assignment was made from density functional theory (DFT) shift calculations that indicated that the terminal site F was downfield of the terminal site G.[23,24] Since the oxygens in site F remain symmetrically equivalent after the single Ti(IV) substitution, it is clear that

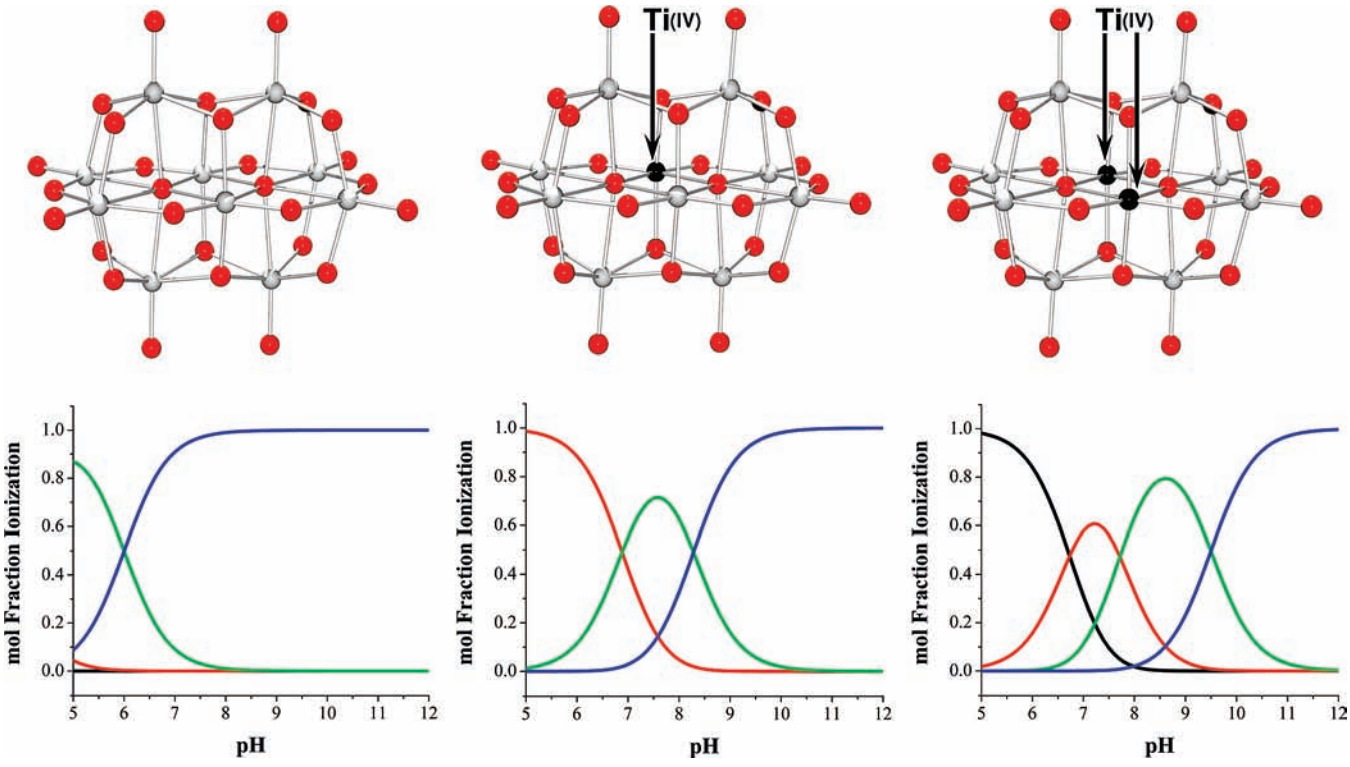

Figure 2. All three isostructural decametalates are shown above their respective acid−base speciation diagrams. From left to right, the ions are the Nb_{10}, $TiNb_9$, and Ti_2Nb_8 ions, where oxygen atoms are shown in red, niobium atoms are shown in gray, and titanium atoms are shown in black. Below the ions are their respective acid−base speciation diagrams, which are shown from pH 5 to pH 12 for clarity and are not meant to infer the stabilities of the ions. For all three plots, the blue trace corresponds to the unprotonated species, the green is the singly protonated species, the red trace is doubly protonated species, and the black trace corresponds with the triply protonated species. With substitution of Ti(IV) for Nb(V), the overall charge of the ions increases and the pK_a values gradually increase (Table 1).

Table 1. Estimated Equilibrium Constants for Protonation of the Anions[a]

molecule	pK_{a1}	pK_{a2}	pK_{a3}
$[H_xNb_{10}O_{28}]^{(6-x)-}$	1.6	3.74	6.0
$[H_xTiNb_9O_{28}]^{(7-x)-}$	6.88	8.28	
$[H_xTi_2Nb_8O_{28}]^{(8-x)-}$	6.73	7.72	9.5

[a] The estimated uncertainties are ±0.25 pK_a units for the $TiNb_9$ ion and ±0.15 pK_a units for the Ti_2Nb_8 ion, each of which were titrated in 0.1 M tetramethylammonium chloride with hydrochloric acid and tetramethylammonium hydroxide. Values for the Nb_{10} ion are inferred from studies of the isostructural and isovalent decavanadate $[H_xV_{10}O_{28}]^{(6-x)-}$ ion via ^{51}V NMR and potentiometry at $I = 0.6$ M.[15]

the previous assignment of the downfield ^{17}O NMR peak position to site G was correct.

The Brønsted acidities of the molecule reflects the −7 charge on the $TiNb_9$ molecule, which is intermediate between the Nb_{10} ion and the Ti_2Nb_8 ion. Titrimetry indicates that there are three protonation states in the $TiNb_9$ ion, and the systematic substitution of Ti(IV) for Nb(V) causes the pK_a's to shift to more alkaline pH's (Figure 2 and Table 1). As was seen for the Nb_{10} ion, but unlike the case for the Ti_2Nb_8 ion, there are no conspicuous broadenings or shifts of the ^{17}O NMR peaks that allow us to confidently assign the protons to individual oxygens. For the Ti_2Nb_8 ion, ^{17}O NMR shifts and line broadenings for signals corresponding to oxygen sites D and E were found around pK_{a1} and pK_{a2}; however, these shifts are missing for both the Nb_{10} and $TiNb_9$ ions. DFT calculations indicate that the highest proton affinities for the $TiNb_9$ ion are at sites B and F, respectively (see Supporting Information), although proton affinities are within 10 kJ/mol of each other for several oxygen sites and thus are not particularly helpful in assigning protonation sites; rather, they suggest that several oxygens may be affected.

The ^{17}O NMR signals for all 11 structural oxygens could be identified in the spectrum, and the intensities diminish as they exchange with the isotopically normal bulk water. As with the Nb_{10} and Ti_2Nb_8 ions, the most rapidly exchanging structural oxygens were the terminal oxygens (sites G_{Ti}, G_{Nb}, and F) and the μ_2-oxo site D. These are followed in reactivity by the μ_2-oxo site on the corners of the molecule, site C_{Ti} and C_{Nb}. Finally, the μ_2-oxo sites E_{Nb} and E_{Ti} are the slowest to react, and rates are shown in Table 2 (see Supporting Information for ^{17}O NMR stacked plots).

The order of reactivities of the various structural oxygens is virtually the same for all three isostructural decametalate ions: Nb_{10}, $TiNb_9$, and Ti_2Nb_8. As was found for site B in the Ti_2Nb_8 ion, there is no evidence that the μ_3-oxo, sites B_{Nb} and B_{Ti}, in the $TiNb_9$ ion undergo isotopic exchange. This result contrasts with our finding for the Nb_{10} ion, where this μ_3-oxo slowly undergoes isotope exchange. Also, base-enhanced dissociation

Table 2. Experimental Conditions and Rates of Steady Oxygen-Isotope Exchange into Sites in the $TiNb_9$ Ion As Measured by ^{17}O NMR[a]

temp[b] (°C)	pH	$[N(CH_3)_4]_7[TiNb_9O_{28}]$ (mM)[c]	log(k) s^{-1} μ_6-oxo (site A)	log(k) s^{-1} μ_3-oxo (site B_{Nb})	log(k) s^{-1} μ_3-oxo (site B_{Ti})	log(k) s^{-1} μ_2-oxo (site C_{Ti})	log(k) s^{-1} μ_2-oxo (site C_{Nb})
35.5	5.5_7	3.01	−5.82 ± 0.30	−5.66 ± 0.29	−5.67 ± 0.39	−4.40 ± 0.06	−4.66 ± 0.08
35.5	5.9_9	2.02	−7.34 ± 0.08	−7.06 ± 0.07	−7.15 ± 0.10	−4.61 ± 0.03	−4.99 ± 0.04
35.5	6.5_4	2.89				−4.54 ± 0.02	−4.93 ± 0.02
35.5	7.0_5	2.85				−4.90 ± 0.01	−5.26 ± 0.03
35.5	7.4_8	2.91				−5.15 ± 0.02	−5.48 ± 0.03
35.5	7.9_2	2.85				−5.45 ± 0.04	−5.87 ± 0.03
35.5	8.4_8	2.83				−5.80 ± 0.02	−6.32 ± 0.02
35.5	8.9_5	2.95				−6.02 ± 0.04	−6.55 ± 0.03
35.5	9.3_8	2.91				−6.25 ± 0.02	−6.90 ± 0.03
35.5	9.9_6	2.89				−6.37 ± 0.03	−7.23 ± 0.04
35.5	10.3_2	2.89				−6.35 ± 0.03	−7.37 ± 0.04
35.5	10.9_8	2.87				−6.32 ± 0.02	−7.42 ± 0.05
35.5	11.6_5	2.95				−6.27 ± 0.03	−7.52 ± 0.10
35.5	12.4_7	2.91	−6.27 ± 0.03	−6.10 ± 0.03	−6.11 ± 0.05	−5.25 ± 0.03	−5.97 ± 0.04
35.5	13.2_5	3.15	−5.04 ± 0.02	−4.93 ± 0.03	−4.93 ± 0.03	−4.54 ± 0.02	−4.87 ± 0.02

temp[b] (°C)	pH	$[N(CH_3)_4]_7[TiNb_9O_{28}]$ (mM)[c]	log(k) s^{-1} μ_2-oxo (site D)	log(k) s^{-1} μ_2-oxo (site E_{Nb})	log(k) s^{-1} μ_2-oxo (site E_{Ti})	log(k) s^{-1} η=O (site F)	log(k) s^{-1} η=O (site G_{Ti})	log(k) s^{-1} η=O (site G_{Nb})
35.5	5.5_7	3.01	−2.55 ± 0.17	−5.20 ± 0.20	−5.23 ± 0.27			
35.5	5.9_9	2.02	−3.00 ± 0.12	−6.62 ± 0.07	−6.73 ± 0.06			
35.5	6.5_4	2.89	−3.55 ± 0.04	−7.44 ± 0.06	−6.54 ± 0.04	−2.68 ± 0.15	−2.95 ± 0.20	−3.02 ± 0.22
35.5	7.0_5	2.85	−4.02 ± 0.04	−7.79 ± 0.10	−6.98 ± 0.04	−3.52 ± 0.12	−3.68 ± 0.14	−3.41 ± 0.18
35.5	7.4_8	2.91	−4.24 ± 0.01	−7.49 ± 0.06	−7.25 ± 0.06	−3.79 ± 0.05	−3.88 ± 0.08	−3.66 ± 0.13
35.5	7.9_2	2.85	−4.33 ± 0.02	−6.66 ± 0.04	−8.03 ± 0.21	−3.47 ± 0.08	−3.59 ± 0.18	−3.39 ± 0.19
35.5	8.4_8	2.83	−4.54 ± 0.01	−6.77 ± 0.03	−8.31 ± 0.40	−3.70 ± 0.07	−3.77 ± 0.04	−3.51 ± 0.06
35.5	8.9_5	2.95	−4.81 ± 0.03	−8.20 ± 0.70		−4.95 ± 0.04	−5.22 ± 0.10	−4.86 ± 0.07
35.5	9.3_8	2.91	−4.88 ± 0.02	−8.11 ± 0.20		−5.25 ± 0.03	−5.46 ± 0.07	−5.10 ± 0.08
35.5	9.9_6	2.89	−4.87 ± 0.03			−5.47 ± 0.05	−5.66 ± 0.13	−5.16 ± 0.12
35.5	10.3_2	2.89	−4.79 ± 0.02			−5.52 ± 0.07	−5.57 ± 0.10	−5.18 ± 0.09
35.5	10.9_8	2.87	−4.53 ± 0.02			−5.56 ± 0.09	−5.56 ± 0.19	−4.78 ± 0.05
35.5	11.6_5	2.95	−4.47 ± 0.03			−5.61 ± 0.09	−5.26 ± 0.17	−4.88 ± 0.15
35.5	12.4_7	2.91	−3.15 ± 0.10	−5.62 ± 0.06	−6.14 ± 0.04	−4.97 ± 0.05	−4.27 ± 0.06	−3.29 ± 0.10
35.5	13.2_5	3.15	−2.48 ± 0.20	−4.77 ± 0.03	−4.95 ± 0.03	−4.42 ± 0.04	−3.61 ± 0.21	−2.08 ± 0.16

[a] The rates were estimated by fitting the time evolution of the signal intensities to an exponential decay.[23,24] Rates corresponding to site A, the μ_6-oxo, indicate the rate at which the $TiNb_9$ ion is reacting to form the new molecule. Rates of the sites G_{Ti}, G_{Nb}, and F were too fast to be estimated at pH ≤6.0 at 35.5°C. [b] Uncertainties in temperature are ±0.2°C. [c] Uncertainties in the concentrations are ±1%. Uncertainties are estimated as the error of the regression or the standard deviation of repeated trials, whichever is larger.

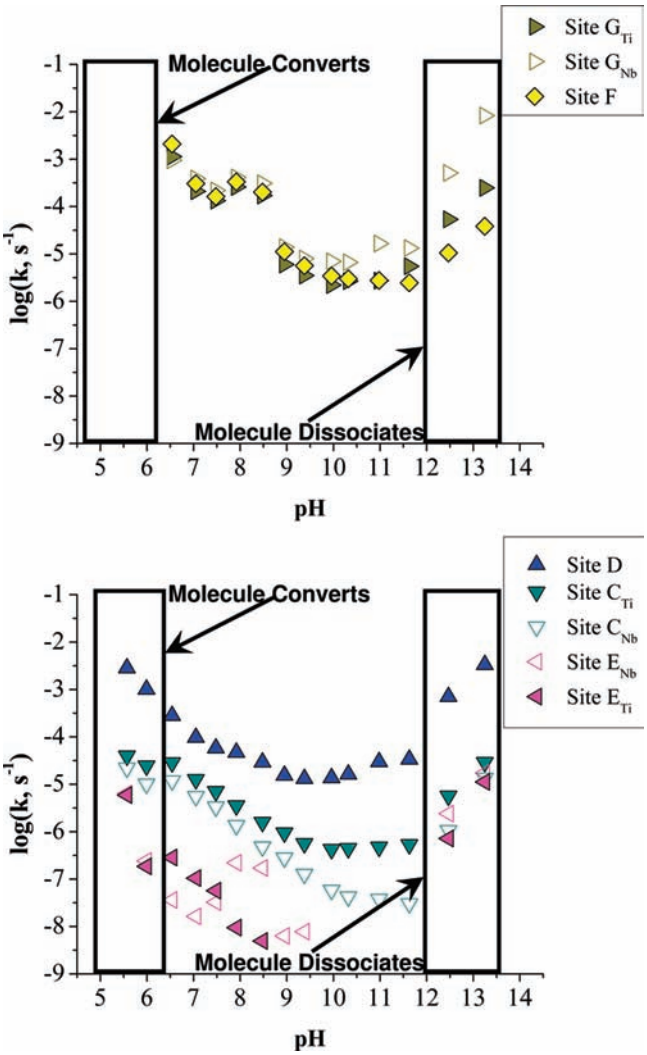

Figure 3. Rates of oxygen exchange for the $TiNb_9$ ion are shown, with the boxed areas indicating where the molecule undergoes side reactions. One can see the effect that this single atom substitution has had on the rates of oxygens that used to be equivalent, which are now labeled with the subscript of Ti or Nb. Top: Rates of isotopic-oxygen exchange for the terminal oxygens of the $TiNb_9$ ion. The rates of exchange increase as the ion protonates and also increase as the ion undergoes base-enhanced dissociation. Rates for the terminal oxygens were too fast to be estimated at pH <6.5. Bottom: Exchange rates for the μ_2-bridging oxygens of the $TiNb_9$ ion are shown. Again, the rates show an increase with protonation and base-enhanced dissociation.

of the Nb_{10} ion became detectable through loss of intensity of site A.[23] As found for all decametalate ions in this series, the central μ_6-oxo, site A, does not exchange with solution unless the molecule is undergoing a side reaction, such as dissociation. At most pH conditions, the ^{17}O NMR intensity for the site A μ_6-oxo is constant, indicating that the molecule is not dissociating.

Examined broadly, the rates of isotopic substitution at most structural oxygens in the $TiNb_9$ ion exhibit an amphoteric chemistry (Figure 3). For sites G_{Ti}, G_{Nb}, and F, the terminal oxygens, rates are relatively fast when the molecule is protonated (pH <9.0) and then drop drastically when the molecule is completely unprotonated (Figure 3, top). As with the Nb_{10} ion, increased base-enhanced isotope exchange rates are associated with slow dissociation of the molecule, as detectable in loss of

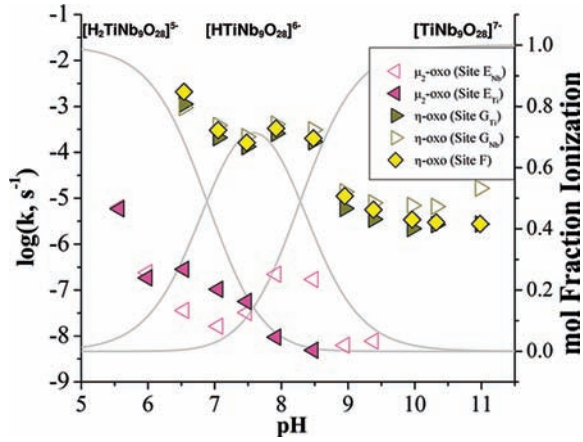

Figure 4. Rates of oxygen exchange for the terminal oxygens sites F, G_{Ti}, G_{Nb}, and μ_2-oxo sites E_{Nb} and E_{Ti} as a function of pH. The speciation diagram is shown in light gray. There is an increase in the rates of oxygen exchange as the pH approaches the highest pK_a (pH ~8.3). Four of the oxygens, sites F, G_{Ti}, G_{Nb}, and E_{Nb}, show this increase and then dramatically drop after the unprotonated species becomes the most dominant (pH ≥9.0). Most interesting is the fact that site E_{Ti} is not affected by this protonation, much in the same way that sites D, C_{Nb}, and C_{Ti} are not affected, while the same oxygen on the titanium side of the molecule (E_{Nb}) is drastically affected.

signal intensity for site A. The oxygen exchange rates for the $TiNb_9$ ion increase at pH ≥12.0 when the molecule slowly dissociates. The reactivity of the μ_2-oxo sites D, C_{Nb}, and C_{Ti} all also show a similar amphoteric trend. Rates of oxygen exchange increase as the molecule becomes protonated (Figure 3, bottom) become relatively insensitive to pH between pH 9.0 and 12.0 (when the molecule is largely unprotonated) and increase in rates at pH ≥12.0 as the molecule begins to dissociate.

The detailed pH dependencies suggest local influences of the Ti(IV) → Nb(V) substitution. In particular, the pH dependencies of the oxygen exchange rates of some oxygens differ depending upon their proximity to the single Ti(IV) → Nb(V) substitution and the protonation state of the molecule. Rates of isotopic exchange in the μ_2-oxo, site E_{Nb}, and the terminal oxygens sites G_{Ti}, G_{Nb}, and F (Figure 4) exhibit a conspicuous "bump" at pH conditions around 8.0 < pH < 9.5 when the $TiNb_9$ ion becomes fully deprotonated. This increase in rates is reproducible and, for site E_{Nb}, is well over an order of magnitude greater than otherwise anticipated. However, on the other side of the molecule, site E_{Ti} exhibits rates of isotopic exchange that steadily decrease with the increase in pH (Figure 4) in the same general amphoteric manner as other oxygens and with no evidence of the bump. In Figure 4, the steep decrease in rates correlates well with the highest pK_a (pH ~8.3). Furthermore, the order of reactivities for the E sites invert with pH: rates trend site E_{Ti} > site E_{Nb} at pH ≤7.5, and site E_{Nb} > site E_{Ti} at pH ≥7.5.

What is striking about the effect of Ti(IV) substitution is that the local effect is so small. Because there is only a single atom replacement in the $TiNb_9$ ion, we can compare the oxygen reactivities at structurally similar sites but that differ in proximity to the central Nb(V) or Ti(IV). The data in Figures 3 and 4 indicate that the structural oxygens (e.g., sites C_{Nb}, E_{Nb}, and G_{Nb} compared to C_{Ti}, E_{Ti}, and G_{Ti}) differ commonly by a factor of ~2−10 for most pH regions.

This variation is similar to that induced by adding sodium as a counterion (see Supporting Information). We probed the

(27) Ohlin, C. A.; Villa, E. M.; Fettinger, J. C.; Casey, W. H. *Angew. Chem., Int. Ed.* **2008**, *47*, 5634.

(28) Gutz, I. G. R. CurTiPot pH and Acid−Base Titration 3.3.2 for Excel; http://www2.iq.usp.br/docente/gutz/Curtipot_.html.

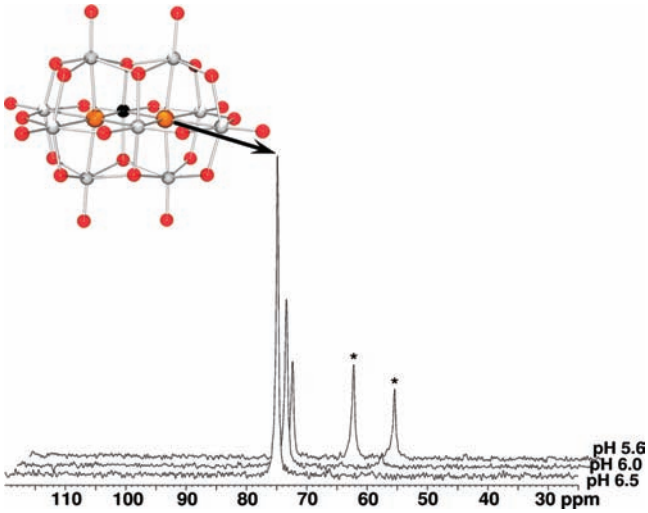

Figure 5. ^{17}O NMR stack plot of the μ_6-oxo for the $TiNb_9$ ion at pH 6.54, 5.99, and 5.57. As the pH decreases, the signal for the μ_6-oxo (site A) shifts and splits from one signal to two new signals, indicated by the asterisks, of nearly equal intensity. The $TiNb_9O$ ion is shown in the upper left with the site A μ_6-oxo shown in orange. The three different spectra are offset for clarity. We speculate that the splitting results from a reaction product forming with two isomers of a single structure, such as a $[H_xTi_2Nb_{18}O_{54}]^{(10-x)-}$ ion with Ti(IV) atoms either on the same side or opposing sides of the ion.

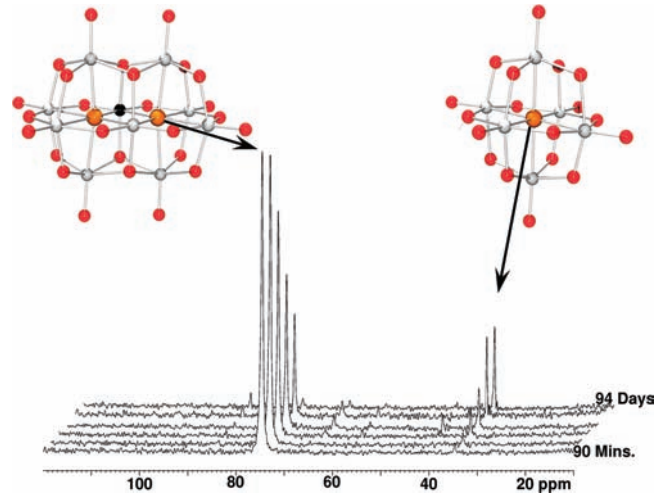

Figure 6. At basic pH conditions, the $TiNb_9$ dissociates to yield a Nb_6 Lindqvist ion, as seen for the Nb_{10} ion.[23] ^{17}O NMR stack plot showing the breakdown of the $TiNb_9$ ion at pH 12.5. The signal for the μ_6-oxo for the $TiNb_9$ ion decreases in intensity with time and, simultaneously, another μ_6-oxo signal grows into the spectra at ~35 ppm. This signal corresponds to the μ_6-oxo for the Nb_6 Lindqvist ion. The $TiNb_9$ ion and the Nb_6 ion are shown on the left and right, respectively, with their site A μ_6-oxo shown in orange.

possible reactivity differences due to counterion effects because our previous experiment on the Ti_2Nb_8 ion employed the sodium salt (in $[N(CH_3)_4]Cl$ background electrolyte), whereas the experiments on the Nb_{10} and $TiNb_9$ ions employed only $[N(CH_3)_4]^+$ counterions and a $[N(CH_3)_4]Cl$ background electrolyte.[23,24] Thus, experiments on the Ti_2Nb_8 ion had eight equivalents of sodium ion that were missing from the comparison studies. The rates for oxygen-isotope exchanges for the tetramethylammonium Ti_2Nb_8 were slightly faster than that of sodium Ti_2Nb_8 under the same pH conditions. The most rapid oxygens (sites F, G, and D) all are faster in the tetramethylammonium Ti_2Nb_8 by approximately a factor of 2 when compared with sodium Ti_2Nb_8. The rates for slower-reacting oxygens (sites C and E) increase in rate by a factor of between 2 and 10 under the same conditions. Ion pairing between polyoxometalates and counterions is unsurprisingly evident in solution; these effects are beyond the scope of the current study and less important than the broad trends in slow isotope exchanges.[29] However, and most importantly, the general order of reactivity for the various structural oxygens in the Ti_2Nb_8 ion remained unchanged by substitution of sodium ion for some of the tetramethylammonium cation.

Two reactions determine the pH limits to decametalate stability. In alkaline solutions, the molecules undergo slow base hydrolysis that, in the case of the Nb_{10} ion, led to formation of the Nb_6 ion.[23] In acid solutions, the conversion products are less clear. For the $TiNb_9$ ion, at pH $\leq$6.0, ^{17}O NMR intensity for site A diminishes with time, indicating that the $TiNb_9$ ion is converting to a new species and not just flocculating into a gel, as it does at pH <5.5. Simultaneously, two new ^{17}O NMR signals growing into the region of the spectrum that is typical for μ_6-oxo in other niobate ions and both are shifted upfield (Figure 5). These new signals are interpreted as peaks corresponding to yet-identified niobate or titanoniobate ions that inherited ^{17}O in a central μ_6-oxo from the reacting $TiNb_9$ ion. These peaks form immediately upon acidification to pH <6.5, indicating that the reaction most likely involves little reorganization and the reaction can also be reversed with quick changes in pH. Attempts to crystallize the product failed.

The rapidity and reversibility of the reaction leads us to suggest that the $TiNb_9$ ion might be dimerizing at the site F oxygens, as was seen by Maekawa et al. for the Nb_{10} ion in nonaqueous solution.[30] The two new upfield ^{17}O NMR signals would then correspond to two isomers of the dimer—one isomer has two Ti(IV) atoms on the same side and the other isomer has the two Ti(IV) atoms located opposite to one another (Figure 5). A similar side reaction at low pH was observed for the Ti_2Nb_8 ions, as well. In acidic solutions, but before precipitation (6.5 < pH < 7.5), the Ti_2Nb_8 ion transforms to yield a single, new signal in the region of the ^{17}O NMR spectrum that is characteristic of μ_6-oxo sites in niobates. The corresponding icosametalate product of acid reaction for the Ti_2Nb_8 ion could be the $[H_xTi_4Nb_{18}O_{54}]^{(12-x)-}$ ion. The icosametalate products could, of course, be intermediates to more condensed structures in the amorphous precipitate, which forms at even lower pH.

The $TiNb_9$ ion is stable above pH 6.5, where the signal from the μ_6-oxo (site A) is constant and remains so until pH $\geq$12.0, where the intensity of the signal from the central μ_6-oxo diminishes slowly with time. In contrast to the reaction at pH <6.5, at pH $\geq$12.0, dissociation of $TiNb_9$ ion is slow. After reaction at pH 12.5, there is distinct evidence of a single major reaction product (Figure 6) with a new μ_6-oxo signal clearly identifiable with the Nb_6 ion, as was also observed in base-enhanced dissociation of the Nb_{10} ion.[23] As the case for the Nb_{10} ion, dissociation of the $TiNb_9$ ion transfers ^{17}O intact to the reaction product (Figure 6).

Discussion

One motivation for undertaking these experiments is to gain insights into how solid oxide surfaces can react with water at a

(29) Antonio, M. R.; Nyman, M.; Anderson, T. M. *Angew. Chem., Int. Ed.* **2009**, *48*, 6136.

(30) Maekawa, M.; Ozama, Y.; Yagasaki, A. *Inorg. Chem.* **2006**, *45*, 9608.

molecular scale. Materials like bromellite (BeO) or corundum (α-Al_2O_3), for example, undergo proton-enhanced dissolution and exhibit a pH dependence that scales with the accumulated surface charge from proton uptake.[31,32] Other oxides dissolve via accumulated negative charge (e.g., SiO_2) or via pH-independent pathways. Many have a broadly amphoteric chemistry where the rates of dissolution increase with both negative and positive charge (e.g., albite, $NaAlSi_3O_8$). The common assumption in simulating these reactions is that the controls on reactivity are local and that capturing an accurate picture of bonding between a detachable metal and its immediate coordination sphere is key.[33−35] However, some mixed-composition oxides present an average reactivity to solution for these reactions that suggests a more complicated chemistry.[36,37]

Two key observations for the Nb_{10}, $TiNb_9$, and Ti_2Nb_8 series speak directly to the question about concerted motions in oxygen exchange reactions:

(1) At this nanometer scale, oxygen sites across a given decametalate structure seem to respond similarly to changes in solution pH, even though the various sites differ by $\sim 10^4$ in rates of steady isotopic substitution.
(2) Net Brønsted acidities, which are inversely proportional to anionic charge for the unprotonated molecules, determine both the dominant pathways for isotope exchange and pH region for molecular stability. The Ti_2Nb_8 ion has a higher affinity for protons than the Nb_{10} ion, and these two molecules undergo oxygen-isotope exchange dominantly via proton-enhanced and base-enhanced pathways, respectively. The $TiNb_9$ ion exhibits both pathways, which differ in relative importance with pH.

These two points are manifested in Figure 7, where the averaged rates of oxygen exchange for the rapidly reacting oxygens (sites C, D, G, and F) are shown for all three decametalate ions. As can be seen, rates for the Nb_{10} ion increase with pH at pH >7 (black squares), although this molecule is completely unprotonated in this pH range (Figure 2). The dominant pathway for isotopic exchange increases with pH and is thus base-enhanced. Opposite results are found for the Ti_2Nb_8 ion, where the rates of isotopic exchange steadily decrease with pH for $6 < pH < 12.5$ (Figure 7, blue diamonds**)**. The Ti_2Nb_8 ion is the conjugate base of a weaker acid than the Nb_{10} ion and is thus protonated to pH $\sim$11 (Figure 2). Correspondingly, the most conspicuous pathway leading to isotope exchanges in the Ti_2Nb_8 ion is proton-enhanced, and rates of oxygen exchange decrease with increasing pH. There is no evidence for a base-enhanced pathway.

Thus, the simple Ti(IV) → Nb(V) substitution at the central metal site for the Ti_2Nb_8 ion completely inverts the pH dependencies for isotopic exchanges for all detectable structural oxygens when compared with that from the Nb_{10} ion. The $TiNb_9$ ion, moreover, exhibits pH dependencies that are intermediate between these two other molecules. Rates of isotopic substitution exhibit both proton-enhanced and hydroxide-enhanced pathways (Figure 7, red circles). Causes of the bump in the pH dependencies for some oxygen sites in the $TiNb_9$ clearly relate to local proton labilization that is well posed for simulation.

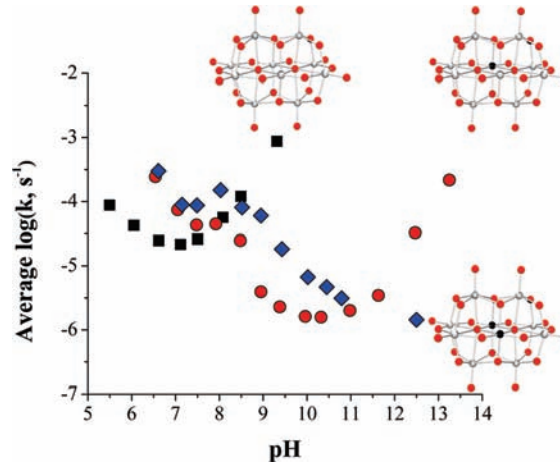

Figure 7. Average rates of oxygen exchange for all fast-reacting oxygens (μ_2-bridging oxygens sites D and C and terminal oxygens sites G and F) for all three isostructural decametalates as a function of pH. Here one can see both the proton- and hydroxide-enhanced pathways for oxygen exchange (boxed regions of side reactions are omitted for clarity). The area of hydroxide-enhanced exchange is shifted toward more alkaline pH when moving from the Nb_{10} ion (black squares) to the $TiNb_9$ ion (red circles); moreover, it seems reasonable to assume that the hydroxide-enhanced region for the Ti_2Nb_8 ion (blue diamonds) is simply shifted too far into the alkaline region to be easily seen. For comparison of individual oxygens across all three molecules, see Supporting Information.

Furthermore, the overall pH stabilities of the molecules also seem to reflect the net molecular charges and acid−base chemistry, indicating a strategy for making particularly pH-stable decametalate versions. The Nb_{10} ion dissociates by hydroxide attack at alkaline pH conditions when the molecule is unprotonated and condenses into an amorphous precipitate at pH <5.0. The base-enhanced pathway for dissociation is absent for the Ti_2Nb_8 ion, which is unstable in acidic solutions and forms an amorphous precipitate at pH <5.5. The $TiNb_9$ ion exhibits enhanced stability at both acidic and alkaline pH conditions when compared with the Ti_2Nb_8 and Nb_{10} ions, respectively (Figure 3), and at pH <5.0 condenses into an amorphous gel.

The strongest argument for equilibrium with metastable intermediates of these decametalate ions comes from the pH dependencies for isotope exchanges discussed above—rates for all structural oxygens within a molecule tend to exhibit very similar pH dependencies, even though the pH dependencies for the different isostructural molecules differ profoundly. Both the Nb_{10} and $TiNb_9$ ions begin to slowly dissociate at higher pH, and all oxygens in these ions respond to the increased [OH^-] concentrations. For these two ions, the rates of oxygen-isotope exchange tend to vary with pH like the rates of dissociation; however, the rates of isotopic exchange are much more rapid than rates of base-induced dissociation. It is difficult to see how all local isotope exchange events would coincidentally have the same pH dependencies as dissociation without having the entire molecule responding as a whole.

The results are consistent with concerted motions of much of the structures during isotope exchange and that a metastable form of the structure serves as a reaction intermediate. In molecular dynamic simulations of the Nb_{10} ion, it was found that [OH^-] nucleophilic attack at the central Nb(V) pulls this metal out of position, allowing solvation of the resulting undercoordinated metal by isotopically normal waters.[24] The substitution of Ti(IV) at this key central metal site stabilizes the

(31) Furrer, G.; Stumm, W. *Geochim. Cosmochim. Acta* **1986**, *50*, 1847.
(32) Koch, G. *Ber. Bunsen-Ges. Phys. Chem.* **1965**, *69*, 141.
(33) Nangia, S.; Garrison, B. J. *J. Phys. Chem. A* **2008**, *112*, 2027.
(34) Morrow, C. P.; Nangia, S.; Garrison, B. J. *J. Phys. Chem. A* **2009**, *113*, 1343.
(35) Lasaga, A. C. *Kinetic Theory in the Earth Sciences*; Princeton University Press: Princeton, NJ, 1998; 728 pp.
(36) Westrich, H. R.; Cygan, R. T.; Casey, W. H.; Zemitis, C.; Arnold, G. W. *Am. J. Sci.* **1993**, *293*, 869.
(37) Casey, W. H.; Ludwig, C. *Rev. Mineral.* **1995**, *31*, 87.

decametalate structure by increasing electrostatic repulsion of the [OH^-] and increasing the electron density at the key μ_3-oxo (site B), thus suppressing the base-enhanced pathway for isotopic exchange of the $TiNb_9$ and Ti_2Nb_8 ions relative to the Nb_{10} ion.

Comba and Helm also suggested that an open intermediate form of the decavanadate ion was key to the observed rates of isotopic exchange.[13] In previous work on the ε-Keggin series of aluminate cations $[MO_4Al_{12}(OH)_{24}(H_2O)_{12}]^{7/8+}$, where M = Al(III), Ga(III), or Ge(IV), it was seen by simulation that a dimer-like moiety forms by partial dissociation of part of the stable structure.[18,38] The extent to which this dimer-like structure forms is strongly affected by the central metal (Al(III), Ga(III), or Ge(IV)) in the inert core of the structure. Thus, single-atom substitutions in the inert core caused variations in isotope exchange rates that span well over $\sim 10^7$ by affecting the formation of a necessary intermediate.

The hypothesis that intermediates are involved in POM reactions is experimentally testable since these structures could conceivably be identified in solution via spectroscopy. The niobates, however, were chosen because they were sufficiently inert to follow the isotope exchanges with ^{17}O NMR. Assuming that the dynamic intermediate reacts extremely quickly once formed, the rate-limiting step must be the formation of this intermediate; therefore, the dynamic intermediate must be present at a small concentration for relatively inert molecules like these niobates. Study of more reactive molecules could present a better chance of identifying an intermediate structure since the steady-state concentrations might be larger. Currently, there is no hypothesis to suggest for the isotope exchange via proton-enhanced pathways, beyond the observation that many of the structural oxygens are affected by a protonation. For all molecules, the site D μ_2-oxo reacts as rapidly as sites F and G, which are η=O, yet the site E μ_2-oxo, which lies in the same equatorial ring as site D, is quite slow.

Enough data now exist on this isostructural series of decametalate ions, however, to look for properties that might correlate with individual site reactivity, even if the molecular details of the exchange mechanisms are unknown. In Figure 8, the κ, which is the formal charge of the oxygen plus the bond valence sum (BVS) for each individual oxygen, is correlated with rates of isotopic exchange at pH ~8.0 for each decametalate ion.[39] The BVS values were calculated using crystal structures of the $[N(CH_3)_4]_6[Nb_{10}O_{28}]$, $[N(CH_3)_4]_7[TiNb_9O_{28}]$, and $[N(CH_3)_4]_8[Ti_2Nb_8O_{28}]$, and no corrections are made for site protonations or hydrogen bonding. The rates show a strong correlation for the bridging oxygens but none for the terminal oxygens, which is not surprising as there is little variation in either rates or κ for these terminal oxygens. However, the correlation shown in Figure 8 does not give any insight into how the overall reactivity of the ion may change with pH. This correlation does suggest that relative rates of oxygen exchange could be predicted by other measures of the electron density on each structural oxygen within a molecule. For example, previous work showed that ^{17}O NMR chemical shifts correlate strongly with oxygen coordination number and the electron density shielding the nucleus.[7,40] In general, the lower the coordination number of the oxygen, the greater the downfield shift of the corresponding peak in the ^{17}O NMR spectrum. Thus, the plot in Figure 8 may give insight into a simple means of estimating rates of isotopic exchange. However, such a correlation may be limited to a particular structural class of POMs.

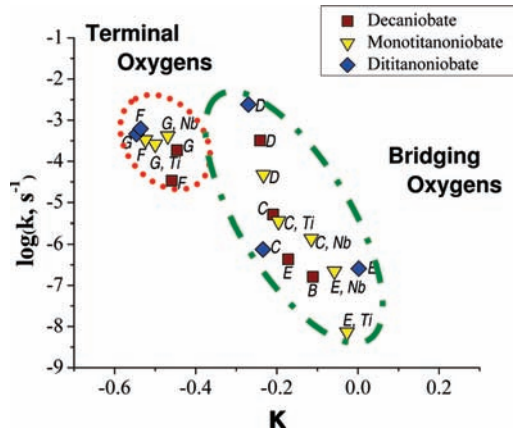

Figure 8. Rate coefficient for isotope exchange is plotted against κ (defined as the formal charge + bond valence sum from the crystal structures). All bridging oxygens here are μ_2-oxygens. The more positive the value for a bridging oxygen, the slower the rate of oxygen exchange. This relationship provides an estimate of relative rates of steady oxygen-isotope exchanges and should be extended to other structures for verification. The BVS values were calculated from the crystal structures of the tetramethylammonium salts of each decametalate, and the rates were taken for all three molecules at pH ~8.0.

Conclusions

The results for these nanometer-size decametalate structures have implications extending beyond the decametalate structural class and, when considered in light of our previous work on aluminum polyoxocations, suggest that concerted motions of the structure have considerable effects on simple oxygen exchange reactions. We find both local and global influences on the reactivities of particular oxygens within a structure. Similarly bonded oxygens within a structure, such as the μ_2-oxos, have large differences in oxygen exchange rates, indicating that the local environments have a big influence on their reactivities. However, within any one of these decametalate ions, rates of isotopic exchange for all sites tend to exhibit similar pH dependencies, indicating that oxygen-isotope exchange pathways involve concerted motions of many atoms, thus showing how the global effects, such as protonation and dissociation, influence the reactivity of most, if not all, oxygens within a structure.

Because the acid−base reactions affect rates for all exchanging oxygens, these structures seem to respond as a unit to changes in pH. For the entire series of ions, Nb_{10}, $TiNb_9$, and Ti_2Nb_8, the relative importance the proton-enhanced or base-enhanced pathways for isotopic exchange tends to reflect the overall charge and hence the proton affinities of the unprotonated molecules. Dissociation at high pH also relates to base-enhanced pathways for isotopic exchanges, so the overall stability of a particular ion in solution also reflects the charge of the unprotonated molecules.

These experimental results aid in our understanding the reactivities of POMs in solution and what controls protonation, stability, and the effects of metal substitutions; moreover, they also help in efforts to accurately simulate reactions at the aqueous−oxide interface. We find that isotope exchange events

(38) Rustad, J. R.; Loring, J. S.; Casey, W. H. *Geochim. Cosmochim. Acta* **2004**, *68*, 3011.
(39) *Bond Valence Sum Calculator*, version 2.00; February 1993, written by C. Hormillosa, with assistance from S. Healy, and distributed by I. D. Brown.
(40) Kidd, R. G. *Can. J. Chem.* **1967**, *45*, 605.

in these nanometer-size ions involve concerted motions of many atoms. The likely pathways involve intermediate forms of the stable structures that are not yet understood. Thus, large dynamic simulations will be indispensable, and the models must be structurally accurate or they can miss the essential chemistry.

Acknowledgment. Support for this research was provided by the National Science Foundation via Grant EAR 0814242 and the U.S. Department of Energy Office of Basic Energy Science via Grant No. DE-FG02-05ER15693. The authors thank Dr. May Nyman (Sandia National Laboratories) for a gift of hydrous niobium oxide and would also like to thank Prof. T. W. Swaddle and Prof. J. Rustad for advice.

Supporting Information Available: Side view of the monotitanoniobate ion, ^{17}O NMR spectroscopy and stacked plots, rate measurements, titration data, electrospray ionization mass spectrometry data, and DFT calculations for all three decametalates. This material is available free of charge via the Internet at http://pubs.acs.org.

JA100490N